AGU PUBLICATIONS

Geophysical Research Letters

RESEARCH LETTER
10.1002/2014GL061157

Key Points:
- Double layers are persistently produced in reconnection
- Double layers moving away from the X line might accelerate electrons on its way
- The electron holes associated with the DLs are gathering toward the X line

Correspondence to:
R. Wang and Q. Lu,
Rongsheng.wang@mail.iggcas.ac.cn;
qmlu@ustc.edu.cn

Citation:
Wang, R., et al. (2014), Observation of double layer in the separatrix region during magnetic reconnection, *Geophys. Res. Lett.*, *41*, 4851–4858, doi:10.1002/2014GL061157.

Received 8 JUL 2014
Accepted 16 JUL 2014
Accepted article online 18 JUL 2014
Published online 28 JUL 2014

Observation of double layer in the separatrix region during magnetic reconnection

Rongsheng Wang[1], Quanming Lu[2], Yuri V. Khotyaintsev[3], Martin Volwerk[4], Aimin Du[1], Rumi Nakamura[4], Walter D. Gonzalez[5], Xuan Sun[6], Wolfgang Baumjohann[4], Xing Li[7], Tielong Zhang[4], Andrew N. Fazakerley[8], Can Huang[2], and Mingyu Wu[2]

[1]Key Laboratory of Earth and Planetary Physics, Institute of Geology and Geophysics, Chinese Academy of Sciences, Beijing, China, [2]Department of Geophysics and Planetary Science, University of Science and Technology of China, Hefei, China, [3]Swedish Institute of Space Physics, Uppsala, Sweden, [4]Space Research Institute, Austrian Academy of Sciences, Graz, Austria, [5]Instituto Nacional de Pesquisas Espaciais, Sao Jose dos Campos, Brazil, [6]School of Physics, University of Science and Technology of China, Hefei, China, [7]Institute of Mathematics and Physics, Aberystwyth University, Aberystwyth, UK, [8]Mullard Space Science Laboratory, Surrey, UK

Abstract We present in situ observation of double layer (DL) and associated electron measurement in the subspin time resolution in the separatrix region during reconnection for the first time. The DL is inferred to propagate away from the X line at a velocity of about ion acoustic speed and the parallel electric field carried by the DL can reach −20 mV/m. The electron displays a beam distribution inside the DL and streams toward the X line with a local electron Alfvén velocity. A series of electron holes moving toward the X line are observed in the wake of the DL. The identification of multiple similar DLs indicates that they are persistently produced and therefore might play an important role in energy conversion during reconnection. The observation suggests that energy dissipation during reconnection can occur in any region where the DL can reach.

1. Introduction

Magnetic reconnection is a fundamental plasma process which converts magnetic energy into plasma energy in the form of bursty bulk flows, heating, and energetic particles, and is believed to be the driver of many explosions in space, astrophysical, and laboratory plasmas. Theoretical and experimental works have already shown that various microphysical processes in the separatrix region play an important role in particle acceleration and energy dissipation [*Matsumoto et al.*, 2003; *André et al.*, 2004; *Pritchett and Coroniti*, 2004; *Drake et al.*, 2005; *Wygant et al.*, 2005; *Retinò et al.*, 2006; *Lu et al.*, 2010; *Mozer and Pritchett*, 2010; *Divin et al.*, 2012; *Wang et al.*, 2012, 2013]. The earlier spacecraft observations have shown that electrons commonly display a field-aligned beam distribution in the separatrix region, and their energy approaches to electron Alfvén speed (a few keV) [*André et al.*, 2004; *Retinò et al.*, 2006] but is less than 10 keV [e.g., *Nagai et al.*, 2001; *Asano et al.*, 2008]. Recent Cluster observations have confirmed that the energy of the inflowing electrons in the separatrix region can reach up to tens of keV [*Asnes et al.*, 2008; *Wang et al.*, 2012, 2013]. This streaming with high energy only persists for a few seconds [*Asnes et al.*, 2008; *Wang et al.*, 2013], and the patchy parallel electric field directed away from the X line is considered to be responsible for the electron acceleration [*Drake et al.*, 2005; *Wang et al.*, 2013]. However, the time resolution of the observed parallel electric field is 1/450 s while the resolution of the electron measurement is 4 s [*Wang et al.*, 2013]. To further confirm the electron acceleration in the separatrix region, the coordinated electric field and electron measurements in the similar time resolution are needed.

The double layer (DL) as a localized, Debye-scale unipolar parallel electric field structure with a net potential provides a physical mechanism for particle acceleration in plasma [*Block*, 1972; *Charles*, 2007]. The spacecraft observations in the auroral region have proved that the DLs are naturally produced and travel along magnetic field roughly at the ion acoustic speed [*Mozer and Kletzing*, 1998; *Ergun et al.*, 2001, 2002]. Recent observations in the magnetotail also present the evidence of the moving DLs in the plasma sheet but without electron measurement [*Ergun et al.*, 2009] and find that all the DLs in the magnetotail are associated with strong magnetic fluctuations. It is still poorly understood why the DLs can be generated in these two distinct plasma environments. In this letter, we report, for the first time, the direct evidence of the DLs moving away from the reconnection X line. Based on the observations, we propose a new mechanism for energy dissipation during reconnection.

©2014. American Geophysical Union. All Rights Reserved.

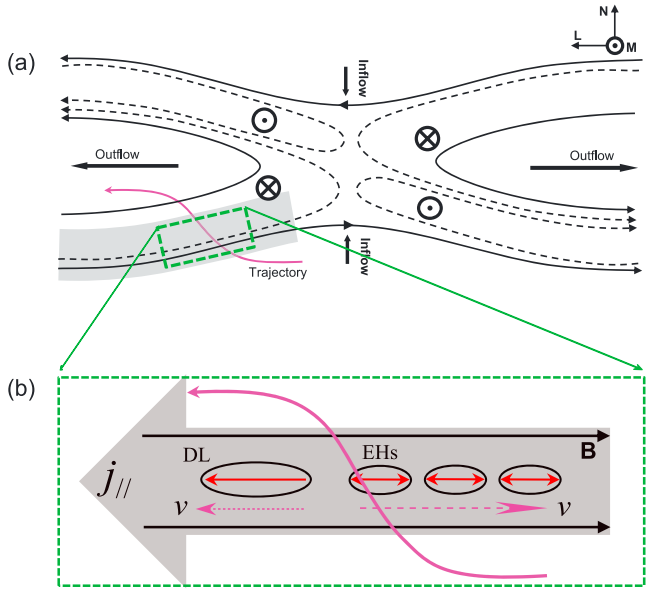

Figure 1. Schematic illustrator of magnetic reconnection diffusion region. (a) Schematic of the reconnection ion diffusion region in the *LMN* coordinates. (b) Electrostatic structures observed within the southern separatrix current layer. The background arrow corresponds to the current layer and the red arrow inside the ellipse is $E_{//}$. The dashed pink arrow denotes the inferred velocities of the electrostatic structures.

2. Observation and Analysis

The magnetic reconnection event encountered by Cluster during 16:35 ~ 17:00 UT on 17 August 2003 is used in this letter to investigate DLs and associated electron distribution in the separatrix region. The reconnection site was retreating tailward at about −18 Earth radii in the magnetotail. This reconnection event with a guide field ($B_g \approx -10$ nT) has been studied in different aspects [*Henderson et al.*, 2006; *Asano et al.*, 2008; *Nakamura et al.*, 2008; *Dai et al.*, 2011; *Wang et al.*, 2013]. The magnetic field, electric field, and ion plasma data are taken from the Flux Gate Magnetometer [*Balogh et al.*, 2001], the Cluster Ion Spectrometry [*Rème et al.*, 2001], and the Electric Field Wave Experiment [*Gustafsson et al.*, 2001] instruments, respectively. The high-energy (>40 keV) electron flux data are taken from the Research with Adaptive Particle Imaging Detectors [*Wilken et al.*, 2001] and the low-energy electron data (27 eV to 23 keV) are obtained from the Plasma Electron And Current Experiment [*Johnstone et al.*, 1997]. The data are shown in a local current sheet coordinate system, which is obtained from the Minimum Variance Analysis applied to the magnetic field during the current sheet crossing (1550–1620 UT) before the reconnection event to avoid the influence of the Hall current system [*Wang et al.*, 2013]. Relative to the geocentric solar magnetospheric coordinates, $L = (0.957, 0.237, -0.166)$ points earthward, $M = (-0.271, 0.935, -0.228)$ points duskside and contains the guide field, and $N = (0.102, 0.263, 0.959)$ directs the current sheet normal, (L, M, N) is a right-handed triple. This coordinates is used throughout this letter except otherwise stated. Here we focus on one southern separatrix region earthward of the X line, as illustrated in Figure 1a.

An overview of the separatrix region crossing is displayed in Figure 2. Cluster traversed the separatrix region from the inflow region to the Hall magnetic field region (Figures 2d and 2g). The separatrix region is characterized by a strong current layer dominated by the parallel component ($j_{//} \approx -60$ nA/m^2, Figure 2e) in the outer boundary of the Hall magnetic field region (Figure 2d) from $T \approx 3$ to 14 s since 16:54:54 UT. The current density is estimated by the Curlometer technique. There are a number of small peaks in the parallel component ($j_{//}$). These small peaks correspond to large magnetic fluctuations and could be caused by the large-scale waves propagating nearly perpendicular to magnetic field [*Dai et al.*, 2011]. As reported in references [*Asano et al.*, 2008; *Nakamura et al.*, 2008], the electron beam with low energy (≤ 10keV) is moving toward the X line along the magnetic field in the separatrix region. By analyzing the high-energy electron data in the same region, we find that energy of the inflowing electrons extends up to 68 keV. Figure 2h displays the electron pitch angle distribution at ~ 68 keV from the satellite of C2. The electron fluxes at ~ 0° are much higher than those at ~ 180° and 90° directions after $T \approx 4$ s. The measurement of energetic electron inflowing is identical to the previous observations [*Wang et al.*, 2013].

During the separatrix region crossing, the data in high time resolution are available because Cluster was in burst mode. The magnetic field and electric field data are sampled at 67 s^{-1} and 450 s^{-1}, respectively. By analyzing all the magnetic field measurements, we find approximate 16 s when the angle between the magnetic field and the spin plane at C2 and C4 is smaller than 5°, i.e., the magnetic field is mainly in the spin plane. In other words, the magnetic field along the spin axis (B_{sa}) is negligible during this 16 s. Therefore, we can calculate the parallel electric field ($E_{//}$) and one component of the perpendicular electric field ($E_{\perp}$) by

©2014. American Geophysical Union. All Rights Reserved.

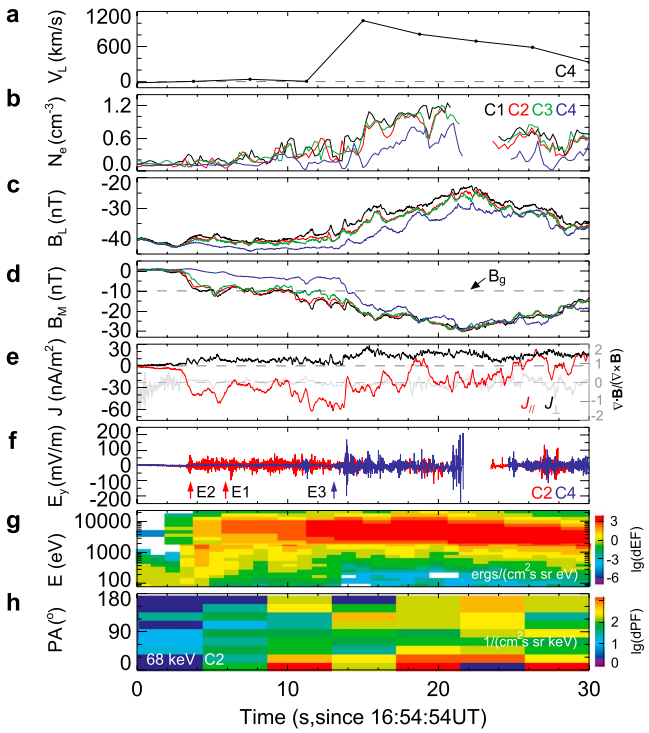

Figure 2. Overview of the electric current layer crossing in the southern separatrix earthward of the X line. (a) Proton burst bulk flow V_L at C4. (b–d) N_e derived from the spacecraft potential, B_L, and B_M (C1: black; C2: red; C3: green; C4: blue). B_g is the guide field, ~ −10 nT. (e) Current density ($j_{//}$ and $j_\perp$) obtained from the Curlometer technique. The gray line is the relative error of $\nabla\cdot\mathbf{B}/(\nabla\times\mathbf{B})$ which are close to zero in the current layer. (f) E_y at C2 and C4 in the Inverted Spin Reference (ISR) system. (g–h) Electron differential energy fluxes for 80 eV to 23 keV and pitch angle distribution of high-energy electrons around 68 keV at C2. The first three vertical arrows in Figure 2f correspond to the events of DLs. The last denotes the event of electron holes. The colors of the arrows signify the corresponding satellites.

assuming $B_{sa} = 0$, although only two components of the electric field in the spacecraft spin plane are measured by Cluster. After examining all the $E_{//}$ data, we find three short periods, in which $E_{//}$ is characterized by a unipolar structure followed by a series of bipolar signatures. The three periods correspond to E1–E3 in Figure 2f. The periods E1 and E2 are observed by C2 and plotted in Figure 3, while the period E3 detected by C4 is displayed in Figure 4. Generally, the Hall electric field directed to the central plasma sheet can be measured in the separatrix region and the typical value is ~ 10 mV/m [*Eastwood et al.*, 2010]. In all three periods E1–E3, the absolute values of B_z are less than 3.5 nT (Figures 3e, 3j, and 4). So the component of the parallel electric field in z direction is only 0.9 mV/m, which is much smaller than the amplitude of the parallel electric field fluctuations in E1–E3 (≥10 mV/m). Therefore, the assumption that magnetic field along the spin axis is equal to zero does not affect our main conclusions.

In the periods E1 and E2, the unipolar $E_{//}$ is negative, and the following bipolar $E_{//}$ pulses is first positive and then negative (Figures 3a and 3f). In the period E1, the duration of the unipolar $E_{//}$ is about 100 ms and the amplitude reaches −20 mV/m. In the period E2, the duration becomes 50 ms and the amplitude of the unipolar $E_{//}$ is ~ −10 mV/m. In both periods, the bipolar $E_{//}$ pulses endure from 10 to 40 ms and are accompanied with the enhancement of $E_\perp$ (Figures 3b and 3g). These bipolar $E_{//}$ pulses display the characteristic of EHs as reported previously [*Matsumoto et al.*, 2003; *Cattell et al.*, 2005; *Khotyaintsev et al.*, 2010]. Moreover, there is a clear gap between the unipolar $E_{//}$ and the turbulence region in the form of EHs in the periods E1 and E2. The signature of a unipolar $E_{//}$ structure followed by a series of EHs is identical to that of the observed DL in the Earth's plasma sheet [*Ergun et al.*, 2009] and in the auroral ionosphere [*Mozer and Kletzing*, 1998; *Ergun et al.*, 2001, 2002]. Therefore, the unipolar $E_{//}$ structures are considered to be the DL in this letter. Although the amplitude of the DL in the period E1 is larger than that in the period E2, the amplitude ratio between DL and EH is the same in both periods. That ratio is about one half.

The propagation velocities of the electrostatic waves in our event cannot be determined directly by interferometry [*Khotyaintsev et al.*, 2010] using the time delay of the signals from two different probes, because individual potentials of the four probes of the electric field and wave experiment (EFW) instrument are unavailable in the burst mode. Suppose that the DLs with a negative $E_{//}$ were moving parallel to the magnetic field, i.e., toward the X line (Figure 1a), the following EHs would be at the low-potential side of the DL. However, this is contrary to the previous observations [*Mozer and Kletzing*, 1998; *Ergun et al.*, 2001, 2002] and the theory [*Newman et al.*, 2001] in which the EHs are verified to be generated at the high-potential side of the DL due to the instability of the electron beam generated by the DL. Hence, we conclude that the DLs in both periods E1 and E2 are propagating antiparallel to the magnetic field (Figure 1b), i.e., moving away

©2014. American Geophysical Union. All Rights Reserved.

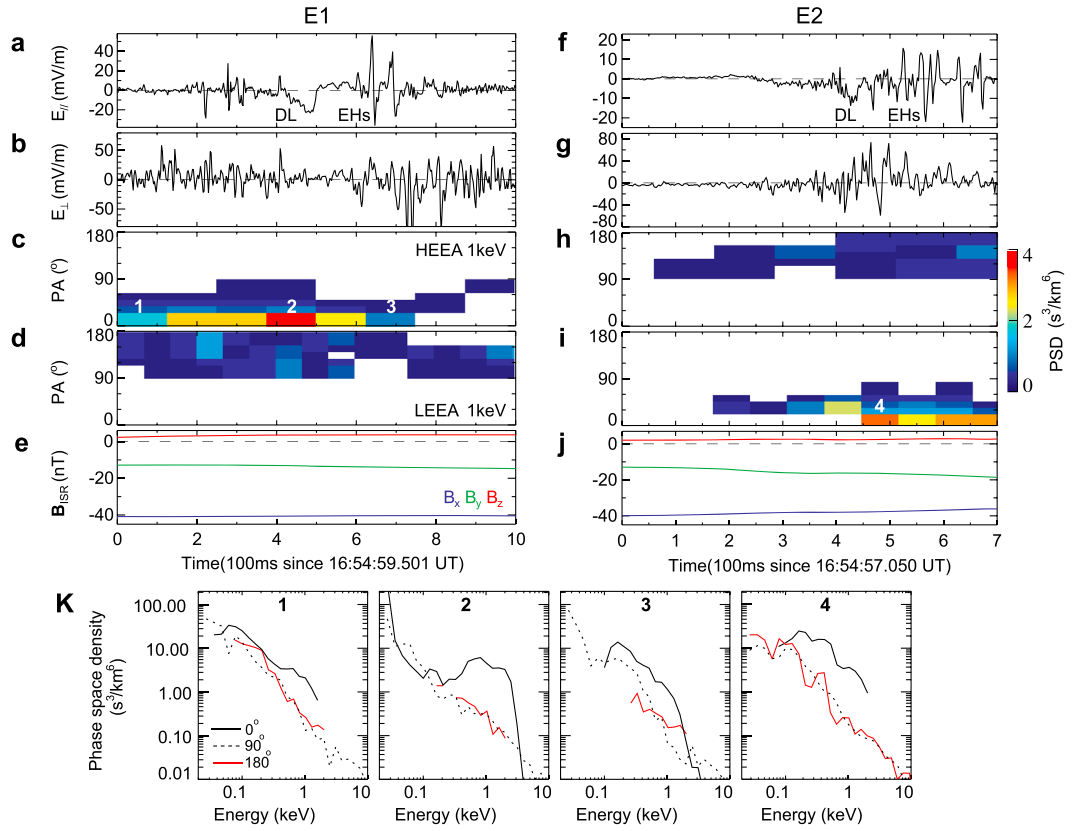

Figure 3. Electrostatic structures and electron pitch angle distribution in the events of E1 and E2. (a–b) $E_{//}$ and one component of $E_{\perp}$ along the axial direction of the spacecraft. The time resolution for the electric field data is 1/450 s. (c–d) Electron pitch angle spectrum from high-energy electron analyzer (HEEA) and low-energy electron analyzer (LEEA) sensors of the Plasma Electron and Current Experiment (PEACE) instrument at 1 keV. (e) B_x, B_y, and B_z in the ISR system, *x-s* plane of which is the spacecraft spin plane. (f–j) The data for E2 are shown in the same format as E1. (k) Slices of electron phase space densities in three components (black: 0°; dashed: 90°; red: 180°) are shown at four different sweep times labeled 1–4 in Figures 3c and 3i. PSD, phase space density.

from the X line. Accordingly, the series of EHs observed in the wake of the DL will be in the high-potential side of the DL (Figures 3a and 3f). The polarity of the EHs is first positive and then negative. Namely, the EHs are propagating parallel to magnetic field, i.e., toward the X line. Consequently, the scenario is that the DL is moving away from the X line in the separatrix region while the EHs in the wake of the DL are propagating toward the X line. This scenario is in accordance to the previous observations and theory. The schematic is shown in Figure 1b. As the DL is moving away from the X line, an electron beam toward the X line would be created. This beam might be the source of the observed EHs in the high-potential side of the DL according to the theory [*Newman et al.*, 2001]. Fortunately, the coordinated electron data associated with the electrostatic waves in the subspin time resolution are available in both periods.

The pitch angle distribution of the electrons from HEEA and LEEA sensors of the PEACE instrument at ~ 1 keV is displayed in Figures 3c and 3d (Figures 3h and 3i) for the period E1 (E2). Each sensor only covers part of the pitch angles. Combining the sweep data of both sensors, the distribution in the full pitch angle range (0°–180°) can be obtained [e.g., *Nakamura et al.*, 2008]. Each color bar in the panels denotes the coverage of the pitch angle for one sweep. The gap means either the sensors do not cover the pitch angle range or no data are collected. The time resolutions for the sweep data from HEEA and LEEA are 118 ms and 58 ms, respectively. This time resolution is comparable to the period of the observed DL. In the period E1, the DL is observed from 400 to 500 ms since 1654:59.501 UT (Figure 3a). Almost simultaneously, one sweep data from HEEA, labeled as 2 in Figure 3c, is collected. The phase space density (PSD) at ~ 0° is significantly larger than those at other pitch angles, and it is also larger than that in the neighboring sweeps (Figures 3c and 3d). The energy spectrum of this sweep data at the three directions (~0°, ~90°, and ~180° relative to magnetic

©2014. American Geophysical Union. All Rights Reserved.

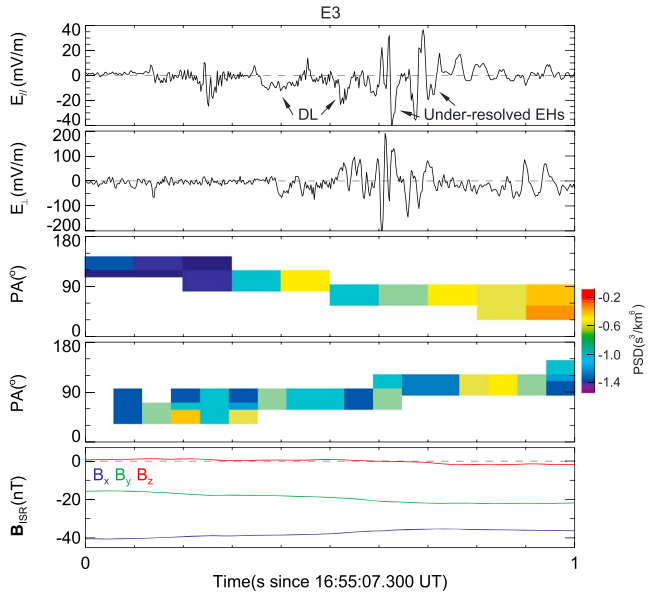

Figure 4. Electrostatic waves observed in the period E3, shown in the same format as E1 and E2.

field) are exhibited in Figure 3k2. It is obvious from Figure 3k2 that there is an intense electron beam parallel to the magnetic field. Its energy is between ~0.4 and ~2 keV. The velocity of this beam is comparable to the local electron Alfvén velocity ($N_e \approx 0.2\,\mathrm{cm}^{-3}$ and $|\mathbf{B}| \approx 40$ nT). The simultaneous occurrence of the unipolar $E_{//}$ and the narrow field-aligned electron beam indicates that the intense electron beam might be generated by the acceleration of the DL.

For comparison, the energy spectrum at other two sweeps is also displayed in Figures 3k1 and 3k3. There two sweeps are measured before and after the DL and are labeled as 1 and 3 in Figure 3c. At these two sweeps, the field-aligned anisotropy is still clear and the phase space density in 0° (black) is higher than those in 90° (dashed) and 180° (red) directions between 0.4 and 2 keV. However, the typical beam distribution becomes less pronounced. This type of field-aligned anisotropic distribution is called electron streaming here. The electron streaming can be observed at the upstream and the downstream of the DL. The energy of the beam within the DL and the energy of the streaming at the upstream as well as the downstream of the DL are consistent (0.4–2 keV). In terms of the beam and streaming energy, it appears that no difference between these regions is observed. That means that the beam within the DL probably does not directly relate to the DL. The maximum energy of the beam and the streaming in these regions is about 2 keV which is nearly equal to the upper limit (2.03 keV) of the LEEA sensor of the PEACE instrument [*Johnstone et al.*, 1997]. So the consistent energy range of the beam observed in these distinct regions is probably caused by the energy limit of the present instrument.

In the period E2, the DL is measured between 400 and 450 ms since 16:54:57.050 UT (Figure 3f). At this time, no electron data parallel to magnetic field is collected. Just after the DL, an electron streaming parallel to magnetic field is observed from 450 to 508 ms (Figures 3h, 3i, and 3k4). This streaming is observed between the DL and the EHs. It covers the energy from 200 eV to 2 keV, even higher. According to the simulations [*Newman et al.*, 2001], the electron streaming can be observed also in the high-potential side of the DL. Therefore, the observed streaming should be directly related to the DL.

In the period E3, the similar $E_{//}$ signature is measured also (Figure 4). However, at least two pulses of the unipolar $E_{//}$ are observed instead of one as in the periods E1 and E2. The amplitudes of the two $E_{//}$ pulses are −10 and −20 mV/m, respectively. It means that there are two separate DLs followed by a series of underresolved EHs. In the period E3, no electron data along magnetic field is collected (Figure 4). In the previous observations [*Ergun et al.*, 2001, 2002, 2009], only one single DL was detected and a series of EHs were measured in the high-potential side of this DL. The two separate DLs have never been observed before. Recently, *Singh et al.* [2011] find that multiple dynamically evolving DLs could be created in their particle-in-cell simulations, which is consistent with our observation in the period E3.

3. Discussion

In the periods E1 and E2, the beam associated with the DL is measured. Suppose the beam within the DL in the E1 was generated by the DL, we can estimate the DL velocity and scale along the magnetic field. In the period E1, the energy of the beam is about 400 eV to 2 keV. This electron beam is measured in the separatrix region. It is reasonable to assume that the electrons are originated from the lobe region, i.e., their initial energy is mostly possible ~100 eV (Figure 2g). Then, the obtained energy of the electrons passing

©2014. American Geophysical Union. All Rights Reserved.

through the DL is ~ 300 to ~ 1900 eV. Namely, the potential drop (ΔU) of the DL is equal to ~300 V to ~ 1.9 kV, which could exceed the electron temperature $T_e \approx 1$ keV in this period E1. The propagation velocity of the DL can be estimated to be $v_{//} = \Delta U/(\Delta t \cdot E_{//}) \approx \sim -150$ to ~ -1000 km/s. This velocity is underestimated due to the usage of the minimum value of the $E_{//}$ (-20 mV/m). This inferred propagation velocity of the DL is comparable to the ion acoustic speed $v_s \approx 800$ km/s (the proton temperature $T_i \sim 8$ keV). The estimated spatial size of the DL along the magnetic field ranges from 12.5 to 62.5$_s$, where λ_D is the electron Debye length ($\lambda_D \approx 1.6$ km).

In the period E2, the observed electron streaming just after the DL covers the similar energy range to that of the beam in the period E1. Given the same assumption that the beam was generated by the DL in the period E2, the potential drop of this DL is roughly consistent with the potential of the DL in the period E1. The amplitude and duration of the DL in the period E2 are half of these in the period E1. Based on the equation $v_{//} = \Delta U/(\Delta t \cdot E_{//})$, the velocity (spatial scale) of the DL in the period E2 will 4 times (twice) the velocity (spatial scale) of the DL in the period E1.

The estimated DL velocity (approximately ion acoustic speed) and spatial scale (tens of electron Debye lengths) along the magnetic field in both periods E1 and E2 are consistent with the previous observation in the auroral ionosphere [*Mozer and Kletzing*, 1998; *Ergun et al*., 2001, 2002]. If the observed DLs in the separatrix indeed propagate at ion acoustic speed as the DLs in the aurora region, then the assumption that the beam is created by the DL is reasonable in a certain degree. However, it does not mean that the beam must be formed by the DL in the periods E1 and E2. The inflowing electron beam is frequently observed in the separatrix region. The simultaneous observation of the beam and the DL in the separatrix region could be just a coincidence.

The DLs are observed for multiple times with the mere 16 s, which indicates that this kind of electrostatic wave is persistently generated during reconnection. According to the analysis above, the potential of a single DL only reaches ~ 2000 V. However, it is still possible for electrons to be energized to tens of keV by passing through numerous DLs. That may be the reason for the inflowing electron with energy up to 68 keV in the separatrix region. However, this speculation cannot be validated at present due to the different time resolution for the high-energy electron (4 s) and the electric field (1/450 s) data. The DL is repeatedly observed in the separatrix region and the electric field of the DL reaches -20 mV/m. This electric field is dramatically larger than the reconnection electric field of about 1.0 mV/m at the X line during steady reconnection [*Vaivads et al*., 2004]. Furthermore, the separatrix region extends substantially wider in the outflow direction than the so-called electron diffusion region. It suggests that energy conversion by the nonlinear electrostatic waves in the separatrix region is significant during reconnection. The intense electric field in reconnection further points out that reconnection in the magnetotail is unsteady as the previous observations [e.g., *Retinò et al*., 2008; *Fu et al*., 2013; *Wang et al*., 2013] and simulations [e.g., *Pritchett*, 2006]. The transient electrostatic waves (DL, EH, etc.) are likely to be associated with the unsteady phase of reconnection.

Numerical simulations proposed that the current is the primary driver for the formation of the DL in the ionosphere and the DL can develop in current-carrying plasma at the site of a density depression [*Newman et al*., 2001]. In our observations, the DLs are indeed observed in the mainly field-aligned current layer along the separatrix region during reconnection. The density depression frequently happens in the separatrix region [*Shay et al*., 2001; *Retinò et al*., 2006; *Lu et al*., 2010; *Divin et al*., 2012; *Zhang et al*., 2012; *Wang et al*., 2012, 2013]. Therefore, the observed DLs in the separatrix could be the current-driven DLs as well. On the other hand, the DLs can be driven also by an externally imposed potential drop along the magnetic field as in laboratory plasma and some numerical simulations [*Singh*, 1982]. The parallel electric field directed away from the X line in the separatrix region has been confirmed [*Wang et al*., 2013]. This parallel electric field could break up into small-scale structures, which is another possible source for the observed DLs. The unique report on the observation of the DL in the magnetotail ($< -10\ R_E$) has confirmed that the DL can be observed in the bursty bulk flow, in the current sheet, and in the plasma sheet boundary and all the observed DLs are associated with strong magnetic fluctuations [*Ergun et al*., 2009]. However, the relation between the observed DL and the reconnection X line has not been resolved there. In this letter, we established that the DLs are persistently created and propagating away from the X line. The strong magnetic and electric fluctuations are always measured around the reconnection site. It is still an issue whether the observed DLs in the magnetotail are all associated with reconnection.

©2014. American Geophysical Union. All Rights Reserved.

Three-dimensional particle simulations have shown that the nonlinear wave of electron holes might play an important role in the electron acceleration during reconnection. The anomalous resistivity is enhanced by the holes scattering electrons [*Drake et al*., 2003]. Such holes have been observed near the outer edge of the current sheet [*Matsumoto et al*., 2003; *Cattell et al*., 2005] and near the center of flux rope [*Khotyaintsev et al*., 2010] in the vicinity of the reconnection X line. The holes in the center of flux rope (slow EHs) are moving much slower than these observed in the outer boundary of the current sheet [*Khotyaintsev et al*., 2010]. All these holes are associated with the narrow electron beam. In our event, the series of EHs in both periods E1 and E2 are accompanied with an inflowing electron streaming instead of an intense electron beam. This is a slightly different from the previous observations. The period of the EHs is about 10–40 ms while the time resolution of the electron data is about 50–100 ms. Thus, the electron distribution within EHs cannot be accurately measured at present. After each DL in our event, a series of EHs moving toward the X line are observed. Namely, a lot of EHs are gathering toward the localized X line region. As suggested by Treumann and Baumjohann recently, electron holes, when created in large number, represent a gas of positively charged quasi-particles [*Treumann and Baumjohann*, 2012]. These EHs gathering toward the X line might form a gas consisting of quasi-particles of such holes therein if the EHs can retain for a while. Then, this gas presumably contributes to the anomalous resistivity by scattering electrons.

The spin time resolution of the spacecraft in orbit is about a few seconds which is too low to resolve the electron acceleration and energy dissipation during reconnection. In this letter, we used the data in the subspin time resolution (2.2 and 100 ms for electric field and electron measurement, respectively) to explore microphysics during reconnection. This kind of data is only available when Cluster is in burst mode. Thus, the chance is very rare. This work shows the first clue to understand the role of the DL during reconnection and also raises a lot of issues, e.g., how the DLs are formed and how long they survive, and what the roles of the EHs play during reconnection. More theoretical and experimental efforts are needed to resolve these issues. The upcoming Magnetospheric Multiscale mission of NASA will provide the unprecedented (milliseconds) time resolution data, which will certainly give us a fantastic opportunity to resolve these issues.

4. Summary

In conclusion, we present the direct evidence of the DLs and associated electron data during reconnection in a very high time resolution of ~ 100 ms. These DLs accompanied with a series of EHs are mainly observed in the separatrix region. The DLs are inferred to propagate away from the X line while the series of electron holes are moving toward the X line. Theoretically, the observed EHs might be created by the electron beam due to beam instability. Within one of the double layers, electron pitch angle data are available and an intense electron beam with a local electron Alfvén velocity is indeed measured. The observation of multiple DLs within the short time span indicates that the DLs are continuously created during reconnection. The work provides a new way to understand energy dissipation during magnetic reconnection.

Acknowledgments

R.W. appreciates the help from Mats André and Cecilia Norgren. All Cluster data other than the PEACE data are available at ESA Cluster Active Archive. We thank the FGM, CIS, EFW, RAPID instrument teams, and the ESA Cluster Active Archive. This work is supported by the National Science Foundation of China (NSFC) grants (41104092, 41174122, and 41274144), and by the China Postdoctoral Science Foundation Funded Project (2011M500030 and 2012T50133). This work is supported by the Austrian Science Fund (FWF) I429-N16.

The Editor thanks Alessandro Retino and an anonymous reviewer for their assistance in evaluating this paper.

References

André, M., A. Vaivads, S. C. Buchert, A. N. Fazakerley, and A. Lahiff (2004), Thin electron-scale layers at the magnetopause, *Geophys. Res. Lett.*, *31*, L03803, doi:10.1029/2003GL018137.

Asano, Y., et al. (2008), Electron flat-top distributions around the magnetic reconnection region, *J. Geophys. Res.*, *113*, A01207, doi:10.1029/2007JA012461.

Asnes, A., M. G. G. T. Taylor, A. L. Borg, B. Lavraud, R. W. H. Friedel, C. P. Escoubet, H. Laakso, P. Daly, and A. N. Fazakerley (2008), Multispacecraft observation of electron beam in reconnection region, *J. Geophys. Res.*, *113*, A07S30, doi:10.1029/2007JA012770.

Balogh, A., et al. (2001), The Cluster magnetic field investigation: Overview of in-flight performance and initial results, *Ann. Geophys.*, *19*, 1207–1217, doi:10.5194/angeo-19-1207-2001.

Block, L. P. (1972), Potential double layers in the ionosphere, *Cosmic Electrodyn.*, *3*, 349.

Cattell, C., et al. (2005), Cluster observations of electron holes in association with magnetotail reconnection and comparison to simulations, *J. Geophys. Res.*, *110*, A01211, doi:10.1029/2004JA010519.

Charles, C. (2007), A review of recent laboratory double layer experiments, *Plasma Sources Sci. Technol.*, *16*, R1–R25, doi:10.1088/0963-0252/16/4/R01.

Dai, L., J. R. Wygant, C. Cattell, J. Dombeck, S. Thaller, C. Mouikis, A. Balogh, and H. Reme (2011), Cluster observations of surface waves in the ion jets from magnetotail reconnection, *J. Geophys. Res.*, *116*, A12227, doi:10.1029/2011JA017004.

Divin, A., G. Lapenta, S. Markidis, D. L. Newman, and M. V. Goldman (2012), Numerical simulations of separatrix instabilities in collisionless magnetic reconnection, *Phys. Plasmas*, *19*, 042,110, doi:10.1063/1.3698621.

Drake, J. F., M. Swisdak, C. Cattell, M. A. Shay, B. N. Rogers, and A. Zeiler (2003), Formation of electron holes and particle energization during magnetic reconnection, *Science*, *299*, 873–877, doi:10.1126/science.1080333.

Drake, J. F., M. A. Shay, W. Thongthai, and M. Swisdak (2005), Production of energetic electrons during magnetic reconnection, *Phys. Rev. Lett.*, *94*, 095,001, doi:10.1103/PhysRevLett.94.095001.

©2014. American Geophysical Union. All Rights Reserved.

Eastwood, J. P., T. D. Phan, M. Øieroset, and M. A. Shay (2010), Average properties of the magnetic reconnection ion diffusion region in the Earth's magnetotail: The 2001–2005 Cluster observations and comparison with simulations, *J. Geophys. Res.*, *115*, A08215, doi:10.1029/2009JA014962.

Ergun, R. E., Y. J. Su, L. Andersson, C. W. Carlson, J. P. McFadden, F. S. Mozer, D. L. Newman, M. V. Goldman, and R. J. Strangeway (2001), Direct observation of localized parallel electric fields in a space plasma, *Phys. Rev. Lett.*, *87*, 045,003, doi:10.1103/PhysRevLett.87.045003.

Ergun, R. E., L. Andersson, D. S. Main, Y. J. Su, C. W. Carlson, J. P. McFadden, and F. S. Mozer (2002), Parallel electric fields in the upward current region of the aurora: Indirect and direct observations, *Phys. Plasmas*, *9*, 3685–3694, doi:10.1063/1.1499120.

Ergun, R. E., et al. (2009), Observations of double layers in Earth's plasma sheet, *Phys. Rev. Lett.*, *102*, 155,002, doi:10.1103/PhysRevLett.102.155002.

Fu, H. S., Y. V. Khotyaintsev, A. Vaivads, A. Retinò, and M. André (2013), Energetic electron acceleration by unsteady magnetic reconnection, *Nat. Phys.*, *9*, 426–430, doi:10.1038/nphys2664.

Gustafsson, G., et al. (2001), First results of electric field and density observations by Cluster EFW based on initial months of operation, *Ann. Geophys.*, *19*, 1219–1240, doi:10.5194/angeo-19-1219-2001.

Henderson, P. D., C. J. Owen, A. D. Lahiff, I. V. Alexeev, A. N. Fazakerley, E. Lucek, and H. Reme (2006), Cluster PEACE observations of electron pressure tensor divergence in the magnetotail, *Geophys. Res. Lett.*, *33*, L22106, doi:10.1029/2006GL027868.

Johnstone, A., C. Alsop, S. Burge, P. J. Carter, A. J. Coates, A. J. Coker, A. N. Fazakerley, M. Grande, R. A. Gowen, and C. Gurgiolo (1997), PEACE: A plasma electron and current experiment, *Space Sci. Rev.*, *79*, 351–398, doi:10.1023/A:1004938001388.

Khotyaintsev, Y. V., A. Vaivads, M. Andre, M. Fujimoto, A. Retino, and C. J. Owen (2010), Observations of slow electron holes at a magnetic reconnection site, *Phys. Rev. Lett.*, *105*, 165,002, doi:10.1103/PhysRevLett.105.165002.

Lu, Q. M., C. Huang, J. L. Xie, R. S. Wang, M. Y. Wu, A. Vaivads, and S. Wang (2010), Features of separatrix regions in magnetic reconnection: Comparison of 2-D particle-in-cell simulations and Cluster observations, *J. Geophys. Res.*, *115*, A11208, doi:10.1029/2010JA015713.

Matsumoto, H., X. H. Deng, H. Kojima, and R. R. Anderson (2003), Observation of electrostatic solitary waves associated with reconnection on the dayside magnetopause boundary, *Geophys. Res. Lett.*, *30*(6), 1326, doi:10.1029/2002GL016319.

Mozer, F. S., and C. A. Kletzing (1998), Direct observation of large, quasi-static, parallel electric fields in the auroral acceleration region, *Geophys. Res. Lett.*, *25*, 1629–1632, doi:10.1029/98GL00849.

Mozer, F. S., and P. L. Pritchett (2010), Spatial, temporal, and amplitude characteristics of parallel electric fields associated with subsolar magnetic field reconnection, *J. Geophys. Res.*, *115*, A04220, doi:10.1029/2009JA014718.

Nagai, T., I. Shinohara, M. Fujimoto, M. Hoshino, Y. Saito, S. Machida, and T. Mukai (2001), Geotail observations of the Hall current system: Evidence of magnetic reconnection in the magnetotail, *J. Geophys. Res.*, *106*, 25,929–25,949, doi:10.1029/2001JA900038.

Nakamura, R., et al. (2008), Cluster observations of an ion-scale current sheet in the magnetotail under the presence of a guide field, *J. Geophys. Res.*, *113*, A07S16, doi:10.1029/2007JA012760.

Newman, D. L., M. V. Goldman, R. E. Ergun, and A. Mangeney (2001), Formation of double layers and electron holes in a current-driven space plasma, *Phys. Rev. Lett.*, *87*, doi:10.1103/PhysRevLett.87.255001.

Pritchett, P. L. (2006), Relativistic electron production during driven magnetic reconnection, *Geophys. Res. Lett.*, *33*, L13104, doi:10.1029/2005GL025267.

Pritchett, P. L., and F. V. Coroniti (2004), Three-dimensional collisionless magnetic reconnection in the presence of a guide field, *J. Geophys. Res.*, *109*, A01220, doi:10.1029/2003JA009999.

Rème, H., et al. (2001), First multispacecraft ion measurements in and near the Earth's magnetosphere with the identical Cluster ion spectrometry (CIS) experiment, *Ann. Geophys.*, *19*, 1303–1354, doi:10.5194/angeo-19-1303-2001.

Retinò, A., et al. (2006), Structure of the separatrix region close to a magnetic reconnection X-line: Cluster observations, *Geophys. Res. Lett.*, *33*, L06101, doi:10.1029/2005GL024650.

Retinò, A., et al. (2008), Cluster observations of energetic electrons and electromagnetic fields within a reconnecting thin current sheet in the Earth's magnetotail, *J. Geophys. Res.*, *113*, A12215, doi:10.1029/2008JA013511.

Shay, M. A., J. F. Drake, B. N. Rogers, and R. E. Denton (2001), Alfvenic collisionless magnetic reconnection and the Hall term, *J. Geophys. Res.*, *106*, 3759–3772, doi:10.1029/1999JA001007.

Singh, N. (1982), Double-layer formation, *Plasma Phys. Controlled Fusion*, *24*, 639–660.

Singh, N., S. Araveti, and E. B. Wells (2011), Mesoscale PIC simulation of double layers and electron holes affecting parallel and transverse accelerations of electrons and ions, *J. Geophys. Res.*, *116*, A00K09, doi:10.1029/2010JA016323.

Treumann, R. A., and W. Baumjohann (2012), Magnetic field amplification in electron phase-space holes and related effects, *Ann. Geophys.*, *30*, 711–724, doi:10.5194/angeo-30-711-2012.

Vaivads, A., Y. Khotyaintsev, M. Andre, A. Retinò, S. C. Buchert, B. N. Rogers, P. Decreau, G. Paschmann, and T. D. Phan (2004), Structure of the magnetic reconnection diffusion region from four-spacecraft observations, *Phys. Rev. Lett.*, *93*, 105,001, doi:10.1103/PhysRevLett.93.105001.

Wang, R. S., et al. (2012), Asymmetry in the current sheet and secondary magnetic flux ropes during guide field magnetic reconnection, *J. Geophys. Res.*, *117*, A07223, doi:10.1029/2011JA017384.

Wang, R. S., A. M. Du, R. Nakamura, Q. M. Lu, Y. V. Khotyaintsev, M. Volwerk, T. L. Zhang, E. A. Kronberg, P. W. Daly, and A. N. Fazakerley (2013), Observation of multiple sub-cavities adjacent to single separatrix, *Geophys. Res. Lett.*, *40*, 2511–2517, doi:10.1002/grl.50537.

Wilken, B., et al. (2001), First results from the RAPID imaging energetic particle spectrometer on board Cluster, *Ann. Geophys.*, *19*, 1355–1366, doi:10.5194/angeo-19-1355-2001.

Wygant, J. R., et al. (2005), Cluster observations of an intense normal component of the electric field at a thin reconnecting current sheet in the tail and its role in the shock-like acceleration of the ion fluid into the separatrix region, *J. Geophys. Res.*, *110*, A09206, doi:10.1029/2004JA010708.

Zhang, Q. H., et al. (2012), Inner plasma structure of the low-latitude reconnection layer, *J. Geophys. Res.*, *117*, A08205, doi:10.1029/2012JA017622.

©2014. American Geophysical Union. All Rights Reserved.